Research Article | Vol. 26, No. 10 | 14 May 2018 | OPTICS EXPRESS 13436
Optics EXPRESS

In situ fabricated 3D micro-lenses for photonic integrated circuits

R. THOMAS,[1] J. LI,[2] SAM LADAK,[1] D. BARROW,[2,*] AND P. M. SMOWTON[1]

[1]*School of Physics and Astronomy, Cardiff University, 5 The Parade, Cardiff, CF24 3AA, UK*
[2]*Cardiff School of Engineering, Cardiff University, The Parade, Cardiff CF24 3AA, UK*
[*]*barrow@cardiff.ac.uk*

Abstract: Aspheric astigmatic polymer micro-lenses were fabricated directly onto photonic integrated circuits using two-photon lithography. We observed a 12.6 dB improvement in the free space coupling efficiency between integrated ridge laser pairs with micro-lenses to those without.

OCIS codes: (250.5300) Photonic integrated circuits; (350.3950) Micro-optics; (220.3630) Lenses; (250.5960) Semiconductor lasers; (220.4000) Microstructure fabrication; (200.4650) Optical interconnects.

References and links

1. S. E. Miller, "Integrated optics – an introduction," Bell Syst. Tech. J. **48**(7), 2059–2069 (1969).
2. L. M. Augustin, R. Santos, E. den Haan, S. Kleijn, P. J. A. Thijs, S. Latkowski, D. Zhao, W. Yao, J. Bolk, H. Ambrosius, S. Mingaleev, A. Richter, A. Bakker, and T. Korthorst, "InP-Based Generic Foundry Platform for Photonic Integrated Circuits," IEEE J. Sel. Top. Quantum Electron. **24**(1), 1–10 (2018).
3. F. Kish, V. Lal, P. Evans, S. W. Corzine, M. Ziari, T. Butrie, M. Reffle, H.-S. Tsai, A. Dentai, J. Pleumeekers, M. Missey, M. Fisher, S. Murthy, R. Salvatore, P. Samra, S. Demars, N. Kim, A. James, A. Hosseini, P. Studenkov, M. Lauermann, R. Going, M. Lu, J. Zhang, J. Tang, J. Bostak, T. Vallaitis, M. Kuntz, D. Pavinski, A. Karanicolas, B. Behnia, D. Engel, O. Khayam, N. Modi, M. R. Chitgarha, P. Mertz, W. Ko, R. Maher, J. Osenbach, J. T. Rahn, H. Sun, K.-T. Wu, M. Mitchell, and D. Welch, "System-on-Chip Photonic Integrated Circuits," IEEE J. Sel. Top. Quantum Electron. **24**(1), 6100120 (2018).
4. S. J. B. Yoo, B. Guan, and R. P. Scott, "Heterogeneous 2D/3D photonic integrated Microsystems," Microsystems Nanoengineering **2**(1), 16030 (2016).
5. N. Lindenmann, G. Balthasar, D. Hillerkuss, R. Schmogrow, M. Jordan, J. Leuthold, W. Freude, and C. Koos, "Photonic wire bonding: a novel concept for chip-scale interconnects," Opt. Express **20**(16), 17667–17677 (2012).
6. X. J. Liang, A. Q. Liu, C. S. Lim, T. C. Ayi, and P. H. Yap, "Determining refractive index of single living cell using an integrated microchip," Sens. Actuators A Phys. **133**(2), 349–354 (2007).
7. S. Cran-McGreehin, T. F. Krauss, and K. Dholakia, "Integrated monolithic optical manipulation," Lab Chip **6**(9), 1122–1124 (2006).
8. S. W. Kettlitz, S. Valouch, W. Sittel, and U. Lemmer, "Flexible planar microfluidic chip employing a light emitting diode and a PIN-photodiode for portable flow cytometers," Lab Chip **12**(1), 197–203 (2012).
9. R. Thomas, A. Harrison, D. Barrow, and P. M. Smowton, "Photonic integration platform with pump free microfluidics," Opt. Express **25**(20), 23634–23644 (2017).
10. G. Williams, M. Hunt, B. Boehm, A. May, M. Taverne, D. Ho, S. Giblin, D. E. Read, J. Rarity, R. Allenspach, and S. Ladak, "Two-photon lithography for 3D magnetic nanostructure fabrication," Nano Res. **11**(2), 845–854 (2018).
11. M. Malinauskas, M. Farsari, A. Piskarskas, and S. Juodkazis, "Ultrafast laser nanostructuring of photopolymers: A decade of advances," Phys. Rep. **533**(1), 1–31 (2013).
12. P. I. Dietrich, R. J. Harris, M. Blaicher, M. K. Corrigan, T. M. Morris, W. Freude, A. Quirrenbach, and C. Koos, "Printed freeform lens arrays on multi-core fibers for highly efficient coupling in astrophotonic systems," Opt. Express **25**(15), 18288–18295 (2017).
13. T. Gissibl, S. Thiele, A. Herkommer, and H. Giessen, "Two-photon direct laser writing of ultracompact multi-lens objectives," Nat. Photonics **10**(8), 554–560 (2016).
14. M. Sartison, S. L. Portalupi, T. Gissibl, M. Jetter, H. Giessen, and P. Michler, "Combining in-situ lithography with 3D printed solid immersion lenses for single quantum dot spectroscopy," Sci. Rep. **7**, 39916 (2017).
15. S. Fischbach, A. Schlehahn, A. Thoma, N. Srocka, T. Gissibl, S. Ristok, S. Thiele, A. Kaganskiy, A. Strittmatter, T. Heindel, S. Rodt, A. Herkommer, H. Giessen, and S. Reitzenstein, "Single Quantum Dot with Microlens and 3D-Printed Micro-objective as Integrated Bright Single-Photon Source," ACS Photonics **4**(6), 1327–1332 (2017).

#315534 https://doi.org/10.1364/OE.26.013436
Journal © 2018 Received 9 Jan 2018; revised 28 Mar 2018; accepted 3 Apr 2018; published 10 May 2018

Optics EXPRESS

16. Z. N. Tian, L.-J. Wang, Q. D. Chen, T. Jiang, L. Qin, L.-J. Wang, and H. B. Sun, "Beam shaping of edge-emitting diode lasers using a single double-axial hyperboloidal micro-lens," Opt. Lett. **38**(24), 5414–5417 (2013).
17. R. I. Handin, S. E. Lux, and T. P. Stossel, *Blood: Principles and Practice of Hematology*, 2nd ed. (Lippincott Williams and Wilkins, 2003).
18. A. Marino, J. Barsotti, G. de Vito, C. Filippeschi, B. Mazzolai, V. Piazza, M. Labardi, V. Mattoli, and G. Ciofani, "Two-Photon Lithography of 3D Nanocomposite Piezoelectric Scaffolds for Cell Stimulation," ACS Appl. Mater. Interfaces **7**(46), 25574–25579 (2015).

1. Introduction

The integration of multiple optical components, on a monolithic substrate to form photonic integrated circuits (PICs) has long been seen as a logical progression following developments in electronics [1]. Recent progress includes the development of generic foundry processes, with Multi Project Wafer users in the healthcare and sensing application areas, as well as in the more conventional, tele- and data-communications [2]. The scale of photonic integration has currently reached a position, where 100's of optical functions, in a system on chip for data communications applications, are commercially deployed, and greater than 1700 optical functions have been demonstrated in the research laboratory [3]. Integration has proceeded in 2-dimensional (2D) structures, and also in 3-dimensional (3D) structures, which consist of stacks of 2D structures [4]. Increasingly large numbers of optical interconnects are required between structures and for general input / output. This demand is soon expected to exceed what is currently feasible with optical fiber coupling technology, due to the limitations imposed by both, the relatively large size of single mode fibers (< 250 μm), and, the cost and complexity associated with their alignment [5]. A solution may be the use of two-photon lithography to produce so called photonic wire bonding [5]. An alternative method, and in some cases a requirement, is for light to be coupled between elements on the same chip in free space and not enclosed in a waveguide. For example, in particle sensing applications [6–9], light passes from the high refractive index waveguide of the PIC, into a low index medium where it interacts with a particle. Any divergence of the light on leaving the waveguide reduces the efficiency and range over which optical power and information, can be coupled back to in-plane sensing elements on the chip. Furthermore, the rates of divergence in the direction normal to the plane of the device (fast axis) to that parallel to the plane (slow axis), can differ substantially when using active optical elements such as a diode laser. This results in non-ideal, elliptical beam shapes, that are not collimated, and which, for particle sensing applications, demand non-trivial analysis [9].

The same two-photon lithography technique used for photonic wire bonding can be used to create free-form components in a variety of polymer materials and by subsequent processing, metallic materials [10]. By utilizing a combination of a high numerical aperture objective lense and the non-linear two-photon absorption process, two-photon lithography is unique amongst additive manufacturing techniques, in its ability to exceed the diffraction limit of the system, and produce spatial resolution of sub-100 nm [11]. This capability has enabled fabrication of optical grade, micro-scaled components, such as, micro-lens arrays [12], refracting lenses [13] in situ on multi-core fibers, and on vertically emitting, single photon sources [14,15]. Two-photon, lithographically fabricated optics, have also been applied indirectly to edge emitting lasers [16]. This was achieved by fabricating the lenses on a planar sacrificial substrate, separating the lenses from the substrate, and finally positioning them with high precision, relative to the edge-emitting laser [16]. To develop a more manufacturable, wafer-scale solution, the lenses should be formed in situ. However, for any in-plane PIC application, where the required additive micro-optics are in close proximity to existing structures, shadowing of the source light required for exposure of the resist, is a significant problem and, a priori, it is not clear whether such structures can be produced.

In this paper we demonstrate how two-photon, lithographically fabricated micro-lenses can be formed in situ, over deep-etched substrates, for the purpose of enhancing the coupling between monolithically integrated, edge-emitting light sources. These sources should be

Optics EXPRESS

geometrically separated by some 200 μm for the future provision of a fluid-conducting trench, for use in microfluidic, lab–on-a-chip applications in analytical chemistry. We compare the power coupling efficiency of integrated pairs of lasers, with and without micro-lenses, using photo-voltage measurements, and discuss current fabrication limitations of the technique for this application, and the constraints that these place on lens/device design.

2. Materials and methods

The optically active semiconductor material used for the PIC substrate was chosen as it has previously been used for particle detection [9] and is a suitable wavelength to examine blood cells in a fluid flow. The material is comprised of a single, quantum well $Ga_{0.51}In_{0.49}P$, p-i-n diode structure, emitting at a wavelength of 633 nm. 1 mm long, 10 μm wide ridge lasers were patterned into the upper surface of the substrate, using a thermally evaporated Ni etch mask, defined with a PMMA lift-off mask, patterned using electron beam lithography. The ridge lasers were formed by vertically etching 4.3 μm into the substrate using an Ar/Cl_2 Inductively Coupled Plasma (ICP). The ridge structures were planarized with a 5 μm thick layer of Microchem SU-8 3005, and back etched using O_2/CF_4 Reactive Ion Etching plasma, to expose the p-doped capping layer. 10/300 nm Cr/Au layers were thermally evaporated over the ridges to form p-side electrical contacts. The backside of the sample was thinned to a thickness of 100 μm, and 100/28/300 nm thick AuGe/Ni/Au layers were thermally evaporated, to form n-side electrical contacts.

To minimize the footprint of the micro-lenses, an aspheric astigmatic refracting lens design, capable of shaping the laser beam in the both the fast and slow axes, with a single refracting surface, was chosen, Figs. 1(a) and 1(b).

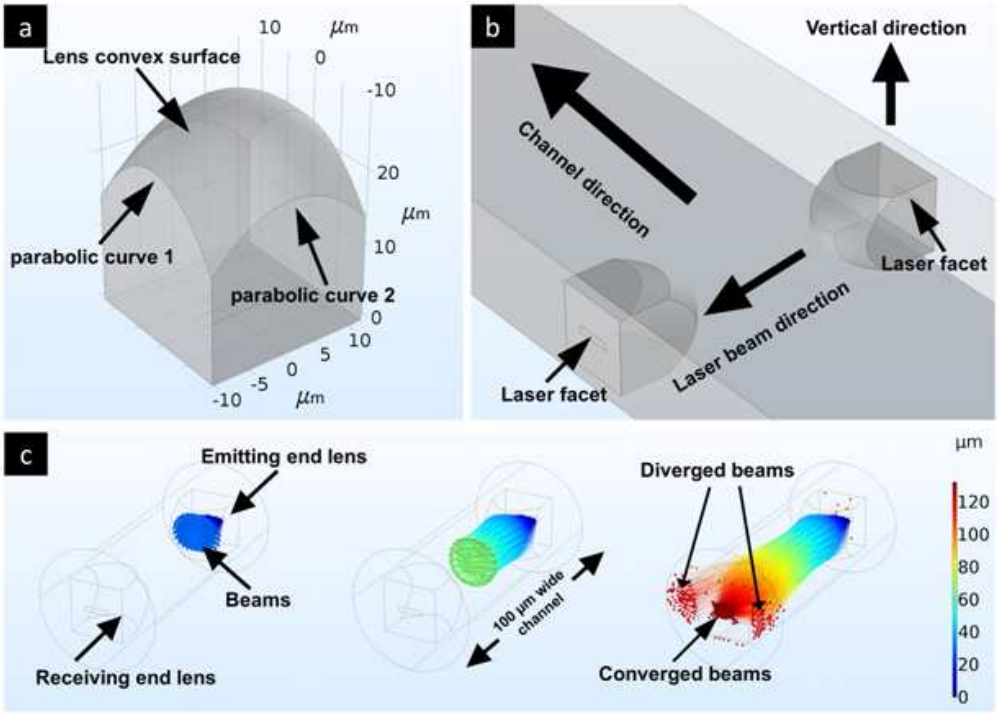

Fig. 1. (a) Schematic diagram of an astigmatic micro-lens design defined by parabolic surface functions. (b) Schema of micro-lenses coupled across a 100-micron wide air-filled channel. (c) Sequential simulation of coupling between lasers with micro-lenses, showing the transformation of an elliptically divergent emitting laser beam into a collimated spot that is focused onto a receiving laser by the second lens. The color line with dot indicates the light path.

Optics EXPRESS

For such a design, the distance from the outer curved surface of the lens, to the light emitting laser facet, determines the spot size of the beam, and, therefore, the minimum horizontal and vertical dimensions that the lens requires, Fig. 1(c). The areal dimension of the lens depends on the required beam size, which for particle sensing is related to the diameter of the particles under scrutiny [9]. For applications examining human blood cells, for example, this would be of the order of 6 – 30 μm [17]. Here we have chosen to produce a beam with a 30 μm diameter spot ($1/e^2$) to illustrate the process but, of course, in principle the approach can be used to tailor beam size for the desired application

In order for the central optical axes of the lens and laser to match, it is necessary for the lower half of the lens to sit within the GaAs substrate. A 20 μm deep trench was etched into the substrate within the 200 μm gap between the laser sections, Fig. 2(a), using a photo-resist mask, and a 5% dilution of H2O2/NH3. The sample was coated in IP-dip photoresist by drop casting, and micro-lenses were fabricated directly onto laser facets, using dip-in, two-photon lithography, with a Nanoscribe GmbH. An added benefit of two-photon lithography is that the facets of the lasers can be buried within the lenses, Fig. 2(b), thus reducing the number of reflecting surfaces between the laser sections and increasing the transmitted optical power.

Vertical alignment of the lenses was achieved by focusing the Nanoscribe microscope at the bottom of the foundation channel prior to writing each lens pattern. Lateral and horizontal positioning of the lenses was carried out by manually aligning the system to a test pattern written on the substrate surface.

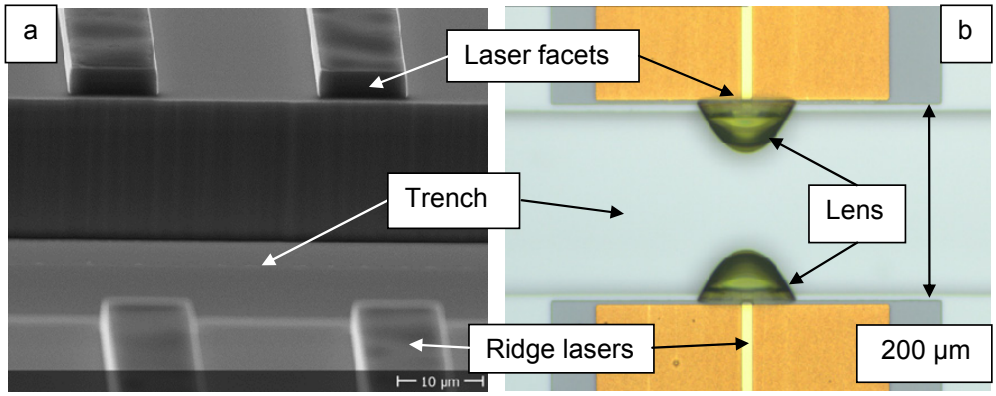

Fig. 2. (a) SEM image of a 20 μm deep trench that was etched into the GaAs substrate between monolithically integrated ridge lasers, to accommodate the 3D micro-lenses. (b) Optical microscopy image of the integrated ridge lasers with facets buried inside mico-lenses.

However, an inherent problem exists for in situ two-photon lithography on pre-structured substrates. Unlike 2D lithographic techniques, in which the exposure is typically performed with normally incident radiation, in two-photon lithography, the light is focused to a small region, a “voxel”, via a high NA objective lens. The exposing radiation is incident from non-normal angles, which are readily obscured, or “shadowed”, by the edges of substrate structures. The loss of intensity and resolution that results, can cause the pattern to become distorted and/or under exposed. From a comparison of the desired lens geometry, in Fig. 1(a), to SEM images taken of fabricated lenses, Fig. 3, several qualitative differences are apparent. For example, the line that appears in the surface of the lens in Fig. 3(a) is a result of the lower half of the lens becoming under exposed, due to the shadowing effect.

Optics EXPRESS

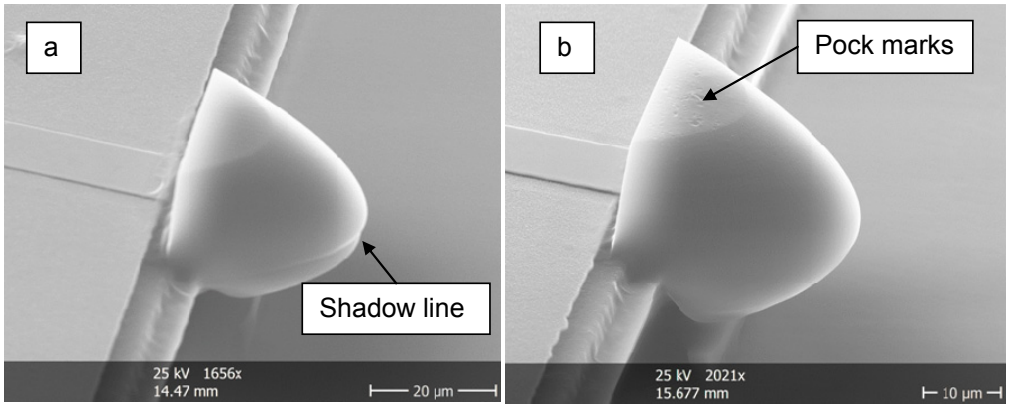

Fig. 3. SEM images of 3D lenses, fabricated using different exposure power scaling (PS) factors, showing a) under exposure of lower half of lens due to shadowing PS = 0.35, and b) pockmarks on the upper surface from vaporization of the resist during over exposure PS = 0.5.

The shadowing effect cannot be avoided, and the problem worsens with the proximity of the voxel to the edge of the structure, and, as the structure's depth is increased. It is possible to compensate for shadowing to some extent, by increasing the exposure dose used, Fig. 3(b). However, an excessive exposure dose could cause the resist to begin to be vaporized, when writing the upper half of the lens, where the shadowing effect does not occur. Vaporization of the resist causes bubbles to form, which can leave pockmarks in the resulting polymerized material Fig. 3(b). This is clearly undesirable for any optical component, as the size of the pock marks could be large enough (> λ) to cause scattering of the light from its surface. An alternative solution is to vary the dose vertically through the pattern, if the two-photon lithography system offers this capability. In this work, the optimal, exposure dose for the lens design was found using an exposure matrix to develop an appropriate process. Optical modelling was undertaken using the ray optics module of the COMSOL Multiphysics software (version 5.3)

3. Results and discussion

Beam divergence angles for the fast and slow axes of the diode lasers were taken from measurements of the laser beam far-field distribution. By approximating the beam profile as Gaussian, $1/e^2$ beam divergence angles of 20° ± 2° and 75° ± 2° were measured for the horizontal and vertical axes respectively, Fig. 4 inset. From these values, the shape and thickness of the lens (the distance from the curved lens surface to the flat end) were calculated for optimal coupling across a 200 µm gap

Lenses with the optimized design were fabricated onto the facets of integrated laser pairs, alongside laser pairs without lenses. We estimate that the error associated with the alignment of the lenses was ± 2 µm in the lateral direction and ± 0.5 µm in the vertical. The fabricated lenses had a surface roughness of less than 50nm (after RF sputter-coating with 20nm Au) as measured with a VEECO Wyco 3300 white light interferometer. The < 50 nm roughness is not surprising given that we set the layer thickness to 150 nm in this study, but which could be set to a lower value. Our previous work has shown via atomic force microscopy, that two-photon lithographic structures can have surface roughness as low as 5nm, though these structures were fabricated at a much slower write speed of 10 µm/s [10]. By operating one of the paired lasers in forward bias, whilst measuring the photo-voltage generated on the opposite laser, the light – current (L-I) characteristics of the emitting laser can be measured by the receiving laser, Fig. 4, and as described in our previous paper [9]. Although these photo-voltage signals are measured in arbitrary units, by taking the ratio of the gradients of the above threshold regions, of the L-I curves for the lensed and non-lensed lasers, a relative

Optics EXPRESS

collection efficiency of the two pairs of lasers can be calculated. From this comparison, we calculate that the coupling efficiency of the lensed pair shows a 12.6 dB improvement. A typical signal to noise value for one of the integrated laser - detectors pairs (without lenses), and with the laser operating at 140 mA and zero bias on the detector, was 10.6. A 12.6 dB improvement in optical coupling due to the lenses therefore results in an SNR of 181. Using the laser beam divergence data, we undertook COMSOL optical simulations of the coupling efficiencies of lasers across a 200 μm trench. Without lenses, the coupling efficiency was 0.90% (–20.5 dB), whereas with the lenses, it was 30.1% (–5.28 dB).

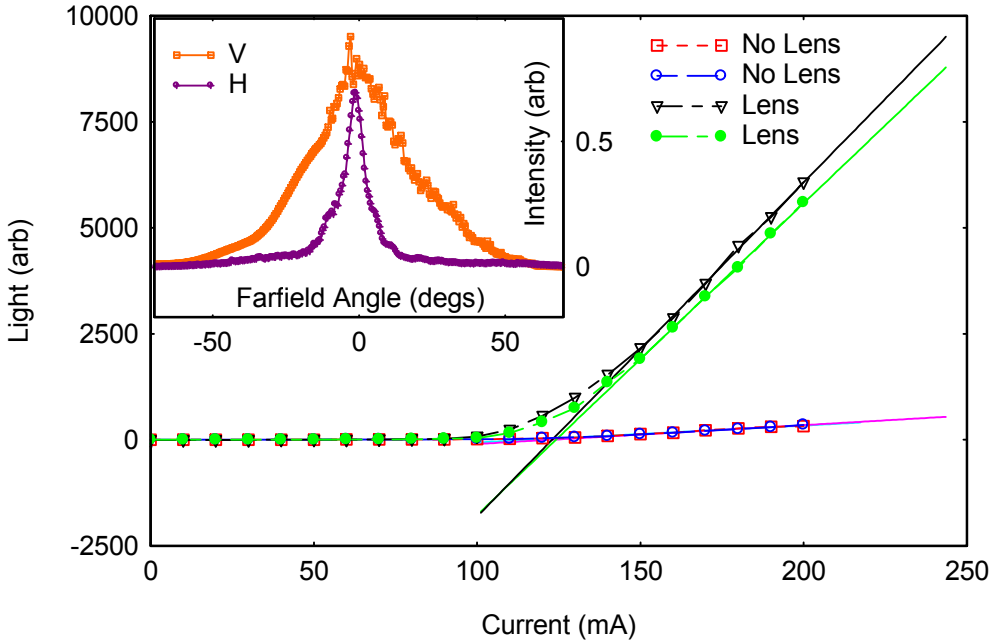

Fig. 4. Light – current characteristics of coupled lasers with micro-lenses (black triangles and green circles) and those without (open blue circles and open red squares). The relative coupling efficiency of the coupled lasers with and without lenses was calculated from the ratio of the gradients of the L-I curves. In each case, the gradients were extracted from the above threshold region of the L-I curve using a straight line fit (solid colored lines.) Inset, far-field distributions for the vertical (orange squares) and horizontal (purple circles) used to determine the fast and slow axis divergence of the ridge lasers, which informed the simulations in Fig. 1.

By extrapolating the above threshold region of the L-I curves to zero on the y-axis, threshold current values were estimated for the lasers and the lasers without lenses. The threshold current values agree within error, which suggests that the addition of the lens may have a negligible effect on the optical feedback to the laser and that the lens surface quality may be such, that any scattered light will be insufficient to change the laser operation. However, spectral linewidth, or relative intensity noise measurements, could provide a more accurate assessment of such potential optical feedback issues, and should be investigated in further studies. This exploratory study demonstrates certain, potential advantages of employing the in situ fabrication of lenses in photonic integrated circuits, namely regarding the issues of alignment, handling and geometrical complexity. However, this potential, needs to be examined much more closely, including issues associated with the economy of the process, for wafer scale processing. The fabrication of a single lens (volume 1.2×10^{-4} mm^3) in this study, using the Nanoscribe two-photon lithography instrument, took 25 minutes, at a write speed of 10 mm/s and 63.8 mW laser power. This is suitable for some prototyping, but clearly insufficient for direct adoption to wafer-scale production. Other issues also arise, such

Optics EXPRESS

as the addition of non-reflective coatings. Furthermore, the alignment of the coupled lenses and the lasers were undertaken manually within the control software of the Nanoscribe, but would require automation in a production scenario. The qualities of the microstructures, such as lenses as produced here, not only depend upon the laser power and writing speed, but also upon the material properties of the photo-resin, which again, needs further research, to develop a diversity of optical qualities, optimised for given applications.

4. Conclusions

Astigmatic aspheric beam shaping micro-lenses have been fabricated in situ on photonic integrated circuits using two-photon lithography. By comparing the light – current characteristics of integrated laser pairs, with and without micro-lenses, we conclude that the free space coupling efficiency is improved by 12.6 dB with our micro-lens design. When performing two-photon lithography over pre-structured PIC substrates, shadowing of the exposing radiation by substrate structures, leads to under exposure of the resulting pattern, which is an effect that must be considered and corrected for at the design stage.

The monolithic integration of such in situ lenses with chip based lasers could play a part in very large scale integration, were a fabrication process available which could overcome the extreme limitations, that are currently inherent in the sequential processing methodology of the direct write technique currently used, and demonstrated here. If such a process were possible, it could possibly be extended to create both sophisticated lens arrays, and actuatable lenses that could be dynamically driven to cater for a diversity of different applications. Such actuation could employ structured piezoelectric nanocomposite resists that have already been demonstrated [18].

Funding

EPSRC grant EP/L005409/1, the National Research Network Wales for advanced engineering and materials (NRN097), funded by the Higher Education Funding Council for Wales and the Welsh Government and funding from the EPSRC (EP/L006669/1 and EP/R009147/1).

Acknowledgments

We gratefully acknowledged the insightful comments from two valuable anonymous referees, whose discussion points have been incorporated into our manuscript. In addition, we gratefully acknowledge the experimental assistance of Andrew Harrison.